Effect of deuteration on phase behaviour of supported phospholipid bilayers

Madrid, Elena; Horswell, Sarah L

DOI:
10.1021/acs.langmuir.5b02765

Document Version
Peer reviewed version

Citation for published version (Harvard):
Madrid, E & Horswell, SL 2015, 'Effect of deuteration on phase behaviour of supported phospholipid bilayers: a spectroelectrochemical study', Langmuir, vol. 31, no. 45, pp. 12544-12551. https://doi.org/10.1021/acs.langmuir.5b02765

Effect of Deuteration on Phase Behaviour of Supported Phospholipid Bilayers: A Spectroelectrochemical Study

Elena Madrid[†] *and Sarah L. Horswell**

School of Chemistry, University of Birmingham, Edgbaston, Birmingham B15 2TT, UK

[†] *Present address: Department of Chemistry, University of Bath, Claverton Down, Bath BA2 7ZA, UK*

*Corresponding author: s.l.horswell@bham.ac.uk

Abstract

Differences in molecular organisation of two sides of a chemically symmetric, planar bilayer supported on a Au(111) substrate have been monitored with charge density measurements and in situ Polarisation Modulation Infrared Reflection Absorption Spectroscopy (PM-IRRAS). Isotopic substitution of the hydrogen atoms in the hydrocarbon chains with deuterium atoms in one monolayer was employed to allow the monitoring of C-H vibrations from that monolayer alone. Charge density measurements of bilayers formed from di-myristoyl phosphatidyl ethanolamine (DMPE) showed that the effect of placing the deuterated layer next to the substrate or electrolyte had little impact on the electrical barrier properties. In situ PM-IRRAS studies revealed that the structure of the two monolayers was the same at negative potentials, where the bilayer is separated from the Au substrate, but different at more positive potentials or small charge densities, where the bilayer is expected to be directly adsorbed on the Au surface. Thus the differences observed for the related molecule di-myristoyl phosphatidyl choline (DMPC) persist in planar structures, although to a lesser extent. A small but observable variation in the tilt angle was also apparent in the spectra of both isotopically asymmetric DMPE bilayers during the electrochemical phase

transition. The fact that this effect was not previously observed for hydrogenous bilayers means that the dynamic behaviour of deuterated DMPE and/or of bilayers composed of different monolayers is different from that of hydrogenous DMPE bilayers. These results have implications for future studies in which isotopic substitution is used to extract selectively information from one layer or component of lipid bilayers in spectroscopic or neutron measurements.

Introduction

Phospholipids are amphiphilic molecules that self-organise in the presence of water to form a range of aggregate structures, the exact natures of which depend on the shape and charge of the constituent molecules.[1] One of these aggregate structures is a bilayer, in which the hydrophilic phospholipid headgroups face outwards to the aqueous phases and the hydrophobic tail groups face the interior of the bilayer, to avoid unfavourable interactions with water. This type of structure forms the basis of biological cell membranes: a phospholipid bilayer matrix, which forms a barrier to ions and polar molecules.[2] Functional molecules, such as ion channel proteins and receptors, are embedded within the lipid matrix and allow the cell to control passage of species through the membrane.[2] Supported lipid bilayers have thus been seen as an attractive model of a biological cell membrane and allow the study of both the mode of interaction of functional proteins and the exploitation of membrane-based receptors as sensors.[3-6]

More recently, the ability to control the electric field across the bilayer whilst simultaneously monitoring changes in bilayer structure have offered a new opportunity to examine membrane processes in detail because it is now possible to study the effects of the electric fields experienced by natural cell membranes.[7-9] Structure and organisation, mechanical properties and solvent content can now all be investigated using in situ infrared

spectroscopy,[8,10-15] scanning tunnelling microscopy,[16,17] atomic force microscopy[18,19] and neutron reflectivity.[9,20] To control the electric field, the lipid bilayer must be supported on an electrode surface. Au(111) is the substrate of choice for in situ structural investigations because it has a wide potential window within which to study non-faradaic processes and is relatively smooth, reducing the amount of defects induced in the lipid bilayer by the substrate.[7,8] Bilayers may be deposited through the fusion of vesicles[8-11, 16, 17-23] or Langmuir-Blodgett techniques,[12-15, 18,19, 24-26] the latter generally resulting in more even distribution of lipids across the substrate and fewer defects in the film. Langmuir-Blodgett (LB) deposition involves the quantitative transfer of a monolayer from the air|liquid interface onto a solid support via the controlled withdrawal of the support through the interface. For the transfer of phospholipid monolayers from water onto Au, this normally results in a monolayer of lipids on Au with their headgroups facing the surface and tailgroups facing out. A second layer, with the new tail groups facing the first layer tail groups, can, in principle, be deposited by lowering the coated substrate back through the monolayer-coated air|water interface, to produce a Y-type bilayer. However this transfer can result in removal of lipids from the first monolayer and so the Langmuir-Schaeffer (LS) method, in which the substrate, now horizontal, is brought into contact with the monolayer, is often preferred.

LB-LS methodology allows for the preparation of asymmetric films, which makes it attractive for studying cell membrane mimics. Real biological cell membranes are asymmetric. The outer monolayer is rich in phosphatidyl cholines (PC), whereas the inner monolayer is rich in phosphatidyl ethanolamines (PE), with a proportion of anionic lipids such as phosphatidyl serines (PS) (see Figure 1).[2,27] The segregation of these lipids across the bilayer is thought to be partly a result of the size of the headgroups, as PE and PS headgroups are smaller than PC headgroups.[2, 27] In this way, curvature of the bilayer is possible. There are also specific interactions between lipid headgroups and other molecules, which may play

a role in their distribution across the bilayer. To obtain a complete picture of the function of a natural cell membrane, it is thus important to understand the physicochemical properties of a range of lipids, organised in different ways.[14,15,20] It is also important to determine the effect of the underlying substrate on the structure of the lipid bilayer.[12] A study of di-myristoyl phosphatidyl choline (DMPC) supported on Au(111) surfaces showed that hydrocarbon chains in the Au-facing leaflet of the bilayer had different tilt angle from the water-facing leaflet of the bilayer. [12] This result was interpreted in terms of an interaction between the headgroup and Au, the headgroup of the Au-facing layer having flatter orientation of the P-N dipole. DMPC, a wedge-shaped molecule, has a natural tendency to curvature, which has an impact on the structure of supported monolayers and bilayers.[16-19] The purpose of the present study was to determine whether differences in molecular orientation across the bilayer persist in planar structures. Di-myristoyl phosphatidyl ethanolamine (DMPE) was selected for investigation because its shape is approximately cylindrical, with the cross-sectional area of two hydrocarbon chains approximately equal in area to its headgroup. DMPE is thus expected to form more easily a planar structure. We measured, under potential control, PM-IRRA spectra of bilayers in which one monolayer comprised per-deuterated DMPE (*d*-DMPE) and the other monolayer comprised hydrogenous DMPE (*h*-DMPE), in order to monitor separately the signals from each monolayer. We compared bilayers in which the deuterated monolayer was deposited first (so adjacent to the Au substrate) with those in which it was deposited second (so adjacent to the electrolyte). We show that the tilt angles of the chains in the two monolayers are practically the same at negative potentials but that there is a slight difference in tilt angle between the two monolayers at potentials positive of the electrochemical phase transition. The small change in tilt angle was not observed for bilayers consisting only of hydrogenous DMPE.[14] Taken together, these results suggest that use of deuterated molecules has a small impact on the

phase behaviour of lipid bilayers, which should be taken into account in future studies in which deuteration is used to shift IR vibrations or to provide contrast in neutron studies.

Experimental

Materials

The lipids di-myristoyl phosphatidyl ethanolamine (*h*-DMPE) and D54-DMPE (*d*-DMPE), in which the two acyl chains have all hydrogen atoms replaced with deuterium atoms, were purchased from Avanti Polar Lipids (Birmingham, AL) and used without further purification. Sodium fluoride (Suprapur grade) was obtained from Merck (VWR) and chloroform and methanol (HPLC grade) were obtained from Sigma-Aldrich. Deuterated solvents used for transmission experiments and deuterium oxide (99.9% D) used for infrared measurements were obtained from Sigma-Aldrich. Water purified with a tandem Elix-Millipore Gradient A10 system (resistivity 18.2 MΩ cm, TOC < 5 ppb, Millipore, France) was used throughout.

Cell preparation

Glassware was cleaned by heating in a mixture of 1:1 nitric and sulphuric acids for at least 1 h, followed by thorough rinsing with ultrapure water and soaking overnight in ultrapure water. Volumetric glassware was cleaned with piranha solution (*Caution! this reaction is exothermic and can cause explosion*) for at least 1 h, followed by thorough rinsing and soaking in ultrapure water. Teflon and Kel-F parts of the spectroelectrochemical cell (along with in-built Au electrode connections) were cleaned with a 1:1 mixture of ammonia and hydrogen peroxide, followed by thorough rinsing and soaking in ultrapure water. The spectroelectrochemical cell was dried, after soaking in ultrapure water, in a specially cleaned oven.

The electrochemical cell was a standard three-electrode cell employing a Au coil (99.997%, Alfa Aesar) as counter electrode and a saturated calomel electrode (Radiometer, Copenhagen), SCE, as reference electrode. The reference electrode was housed in a separate compartment and connected to the main cell via a salt-bridge. The electrolyte used was 0.1 M NaF and the cell was kept free of oxygen by purging with argon before and during measurements. The Au(111) electrode (Mateck, Germany) was prepared by flame annealing as described previously[28] and transferred to the electrochemical cell (and to the Langmuir trough) with a protective drop of ultrapure water, to minimize contamination. The Au(111) electrode used for PM-IRRAS measurements was prepared in a similar way. The CE in the spectroelectrochemical cell was a Au coil, concentric around the WE, and the reference electrode was a Ag|AgCl|3 M NaCl reference electrode (BASi, US). Potentials in this work will be referred to the Ag|AgCl|3 M NaCl reference electrode. The window was a 1″ BaF_2 equilateral prism and was prepared by washing in methanol, rinsing with ultrapure water, drying with nitrogen and placing in an ozone chamber for 30 min. 0.1 M NaF was used as electrolyte in order to suppress the solubility of the window. This electrolyte was prepared in D_2O. Electrochemical and PM IRRAS experiments were performed at 19 °C. At this temperature, DMPE is in the gel phase, as the main chain melting transition occurs at ~50 °C.[29-31] Comparisons of chain melting transitions for lecithins and their deuterated analogues have indicated a decrease of 4-5 °C on deuteration[32] and a small increase of ~0.5 °C is observed for DMPE if D_2O is used as solvent rather than H_2O.[29] Assuming a similar trend can be applied to PE as PC, *d*-DMPE is also in the gel phase at 19 °C and well below the chain melting transition.

Instrumentation

Pressure-area isotherms were recorded on a water sub-phase using a Nima trough (Nima, UK) of area 600 cm^2 equipped with a Delrin barrier and a dipper. A known quantity

(typically 50-60 μL) of a 1 mg mL^{-1} solution of DMPE or *d*-DMPE(prepared in a 9:1 v/v chloroform:methanol mixture) was deposited on the water sub-phase with a microlitre syringe and allowed to equilibrate for 30 min. The monolayer was compressed at a rate of 25 cm^2 min^{-1} (ca 4% of the initial area per minute). To deposit a bilayer on a Au(111) surface, the flame-annealed Au electrode was placed below the surface of the subphase before deposition and compression of the monolayer. The electrode was then withdrawn through the monolayer (Langmuir-Blodgett deposition) at a speed of 2 mm min^{-1} and a fixed surface pressure of 47 mN min^{-1} (at which the molecules exist in the solid phase in each case). The surface was dried in Ar for 30 min and then a second monolayer was formed on the first using a Langmuir-Schaeffer (horizontal dip) deposition method. The electrode was then transferred to the electrochemical cell or dried and transferred to the IR cell, as required.

Electrochemical measurements were made with a Heka PGStat590 potentiostat, connected to a PC via a data acquisition board (M-series, National Instruments) and BNC block. Data were acquired with in-house written software [kindly provided by Dr Alexei Pinheiro, Universidade Tecnologica Federal do Parana, Londrina, Brazil], which also controlled the chronocoulometry experiment. Differential capacity measurements employed a dual channel DSP 7265 lock-in amplifier (Ametek, Germany), connected to the potentiostat. An a.c. signal of amplitude 5 mV and frequency 20 Hz was superimposed on a slow potential sweep (5 mV s^{-1}) and the resulting in-phase and quadrature components of the current analysed to give the capacitance as a function of applied d.c. potential, assuming a series RC circuit. Chronocoulometry measurements were carried out as follows using the procedure described previously.[13-15] Briefly, differential capacitance measurements were used to choose a base potential (in a region of stability for the bilayer) and to determine the potential at which molecules were desorbed. The potential was held at the base potential (–0.06 V) for 60 s, then stepped to the potential of interest and held for 3 min to allow equilibrium to be reached. It

was then stepped briefly to –1.01 V for 0.15 s to desorb all the molecules, during which time a current transient was recorded, and then returned to the base potential. This process was repeated for a series of potentials moving in the cathodic direction from 0.36 V vs SCE, with a step size of 50 mV.

Spectra were acquired with a Bruker Vertex 80v spectrometer, equipped with modified PMA50 module for PM-IRRAS measurements. The photoelastic modulator and controller were from Hinds (U.S.) and the signal was demodulated with a synchronous sampling demodulator, SSD, (GWC Technologies, U.S.) using the technique reported by Corn et al.[33,34] The detector was a liquid nitrogen-cooled mercury cadmium telluride (MCT) detector. For each applied potential, a total of 8000 scans was acquired. A macro within the Bruker OPUS software was used to control the potentiostat. The PEM was set for half-wave retardation at 2900 cm^{-1}, the angle of incidence was 51° and the thickness of solution between the Au surface and the window was around 2 μm. These parameters were chosen to optimize signal in the C–H stretching region, using the calculations reported by Jackson and Zamlynny,[35] and the electrolyte thickness was determined by comparing experimental reflectivity spectra with theoretical spectra, calculated for the cell configuration as described by Zamlynny and Lipkowski.[36] The calculations were carried out with "Fresnel 1" software kindly provided by Prof. V. Zamlynny (Acadia University, Canada).[37]

The intensity average and difference signals were corrected for the response of the PEM with a modification of the method described by Buffeteau et al.,[38] which has been described in detail by Lipkowski et al., along with the method employed for spline interpolation to background-correct the resulting spectra.[39] The background-corrected spectrum plots ΔS, which is related to the absorbance of the adsorbed molecules by:

$$\Delta S = \frac{2\left(I_s - I_p\right)}{I_s + I_p} \approx 2.3\Gamma\varepsilon = 2.3A \qquad (1)$$

where Γ is the surface concentration of the adsorbed species, ε is its molar absorption coefficient and A is the absorbance.[39] Separate transmission IR experiments are needed to evaluate isotropic optical constants of DMPE, which can then be used to simulate PM-IRRA spectra of randomly organised molecules in the spectroelectrochemical cell.[36,39] The transmission spectra were measured in a liquid cell comprising BaF_2 windows separated by a 10 μm Teflon spacer. DMPE is not soluble in water; therefore, a mixed deuterated methanol (CD_3OD)/chloroform ($CDCl_3$) solvent was used for transmission spectra measurements. Software provided by V. Zamlynny[37] was used to calculate isotropic optical constants from the transmission spectra of DMPE. These optical constants were then used to calculate the theoretical PM-IRRA spectra of randomly oriented molecules expected for the cell configurations used in each of the PM-IRRAS measurements. The theoretical spectra were used to calculate the tilt angles of the transition dipole moments of the vibrations with respect to the surface normal.

Results

Monolayers

Figure 2 compares the pressure-area isotherm of per-deuterated di-myristoyl phosphatidyl ethanolamine (*d*-DMPE) with that of the hydrogenous DMPE (*h*-DMPE). The shapes of the isotherms are similar: at higher area per molecule, the molecules are in a gaseous phase, which condenses to an expanded liquid (L_e) phase at ~75–80 $Å^2$. A phase transition to the condensed liquid (L_c) phase is apparent as a practically horizontal region leading into a steeper sloped portion of the isotherm (which corresponds to the L_c phase). Finally, on compressing further, a phase transition to a solid-like phase occurs. The solid phase is characterised by low compressibility, hence a steep slope in this portion of the isotherm. The two molecules reach the same limiting molecular area (~38 $Å^2$) in the solid phase, which is in

agreement with literature values for DMPE.[40] The main difference between the isotherms is seen in the phase transition between the L_e and L_c phases. For a given temperature, the phase transition occurs at a higher surface pressure for *d*-DMPE than for *h*-DMPE. (An alternative view might be that to condense the L_e to L_c phase at a particular pressure, a lower temperature is needed for *d*-DMPE.) This implies that *d*-DMPE has greater fluidity in the liquid phase than *h*-DMPE. This is an interesting result because the isotherms of the related molecules *d*-DMPC and *h*-DMPC are very similar.[12] The reason is not immediately obvious. A similar difference in surface pressure of the L_e-L_c transition has been previously mentioned for D62 DPPC and *h*-DPPC but not discussed in detail.[41,42]Perhaps if one assumes a van der Waals relationship between surface pressure and area in the L_e phase, the result would suggest either that the strength of attractive intermolecular interactions is decreased for *d*-DMPE relative to *h*-DMPE or that the average volume of the molecules is smaller. This latter could occur as a result of smaller amplitude of CD_2 vibrations compared with CH_2 vibrations. The notion is in line with the observations that chain melting transitions occur at lower temperatures for deuterated molecules,[32] which is also indicative of weaker intermolecular interactions.

Electrochemical measurements

Figure 3 presents plots of charge density vs potential (from chronocoulometry measurements) for asymmetric DMPE films on Au(111). The error bars represent a standard deviation over three measurements. The plot compares Au|*d*-DMPE|*h*-DMPE with Au|*h*-DMPE|*d*-DMPE films. Little difference is observed between the electrochemical responses of these films, which suggests that, in the solid phase at least, the macroscopic properties of the films are similar. The charge density values are comparable with similar plots obtained for *h*-DMPE bilayers supported on Au(111).[14] The similarity of the charge-potential plots for each starting structure could also be explained by isotopic scrambling as a result of lipid "flip-flop"

between layers, which has been observed in sum frequency generation (SFG) experiments by Conboy et al.[43-46] In the following discussion we have assumed that isotopic scrambling does not take place to a large extent in our bilayers. In the case of DMPC[12] and in our case (vide infra), the tilt angles derived from C-H stretching modes for bilayers where the hydrogenous molecules were deposited in the electrolyte-facing leaflet were consistently higher than for bilayers where the hydrogenous molecules started adjacent to the Au surface. If the deuterated molecules were evenly distributed across the two layers, the same tilt angle would be expected for both starting structures. The difference between our results and those from SFG experiments probably arises from differences in film preparation. The SFG experiments were carried out on films prepared at higher temperatures (relative to the chain melting transition temperature) and at lower surface pressures, so there is likely to be more flexibility in these bilayers than in the bilayers described herein.

PM-IRRAS measurements

Figure 4 shows a spectrum in the C-H stretching region of a Au|*h*-DMPE|*d*-DMPE film, at an applied potential of 0.0 V. The spectra contain four fundamental modes and two additional Fermi resonances, arising from coupling between CH_2 bending overtones and the symmetric methylene stretching mode.[47-49] The spectrum in Figure 4 can be fitted to show the six components and an example of this fitting, in which the bands have been fitted with mixed Gaussian-Lorentzian character, is provided in Figure 4. The bands at 2851 cm^{-1} and 2919 cm^{-1} correspond to CH_2 symmetric and antisymmetric stretching modes, respectively.[24,30,31,47,48,50-55] The bands at 2874 cm^{-1} and 2963 cm^{-1} correspond to CH_3 symmetric and antisymmetric stretching modes, respectively.[24,30,31,47,48,50-55] These bands are similar in shape and position to those observed for *h*-DMPE bilayers supported on Au(111) surfaces.[14] Figure 5 shows spectra acquired at selected applied potentials for each of the two films. The position of the band provides an indication of the degree of ordering of the

hydrocarbon chains in that an increase in the number of *gauche* conformers results in an increase in wavenumber. [30,47,50,51,52] The band position changes very little as the applied potential is varied and values average at 2851.7 cm^{-1} and 2919.4 cm^{-1} for the CH_2 symmetric and antisymmetric stretching modes, respectively, for the Au|*h*-DMPE|*d*-DMPE film and 2851.2 cm^{-1} and 2919.1 cm^{-1} for the Au|*d*-DMPE|*h*-DMPE film. These values are indicative of a film in which the hydrocarbon chains are in the gel state.[30,47,50,51,52] The close similarity of the band positions for the CH_2 modes in each type of film indicate that placing the *h*-DMPE film adjacent to the surface or to the solution makes little difference to the average conformation of the molecules. The full width half maxima (fwhm) observed (20.2 cm^{-1} and 11.9 cm^{-1} for the antisymmetric and symmetric stretches of the Au|*h*-DMPE|*d*-DMPE film, respectively, and corresponding values of 18.4 cm^{-1} and 11.2 cm^{-1} for the Au|*d*-DMPE|*h*-DMPE film) suggest relatively low mobility of the hydrocarbon chains (a large bandwidth indicates greater mobility).[31] The hydrocarbon chains in the monolayer adjacent to the electrode have only very slightly more mobility than those in the monolayer adjacent to the solution; both films display slightly higher fwhm than symmetric Au|*h*-DMPE|*h*-DMPE layers (16-19 cm^{-1} and 10.5-11 cm^{-1} reported in ref. 15).

Finally, the integrated intensity of the bands reveals information on the orientation of the CH_2 stretching mode transition dipoles, from which the orientation of the backbone of the hydrocarbon chain can be determined.[8,10-15, 36,39] The integrated band intensity is related to the angle between the transition dipole moment and the electric field vector according to Eq 2:

$$\int A\mathrm{d}\nu \;\; \alpha \;\; |\boldsymbol{\mu}.\boldsymbol{E}|^2 = |\mu|^2\langle E\rangle^2\cos^2\theta \qquad (2)$$

where the integral represents the integrated band intensity, μ is the dipole moment, E is the electric field intensity and θ is the angle between the vectors representing these quantities.[39,56] For molecules adsorbed at a metallic surface, the electric field vector may be taken to be perpendicular to the surface and so θ represents the angle made by the transition dipole moment and the surface normal. The intensity is related also to the amount of material present and so the experimental data must be compared with simulated spectra of randomly organised molecules at the surface, using the same experimental parameters (angle, thickness of electrolyte between the surface and the window, thickness of the film). The tilt angle of the dipole moment is then calculated from Eq 3:[39,57,58]

$$\cos^2\theta = \frac{1}{3}\frac{\int_E A\mathrm{d}\nu}{\int_{random} A\mathrm{d}\nu} \qquad (3)$$

where $\int_E A\mathrm{d}\nu$ is the band intensity in the experimental spectrum at a given applied potential and $\int_{random} A\mathrm{d}\nu$ represents the integrated band intensity in the simulated spectrum.

Figure 6 is a schematic diagram of the relationship between the transition dipole moments of the symmetric and antisymmetric stretching modes and the direction of the chain tilt angle. The tilt angle of the hydrocarbon chain is calculated from the tilt angles of the transition dipole moments using Eq 4:[39,59]

$$\cos^2\theta_s + \cos^2\theta_{as} + \cos^2\theta_{chain} = 1 \qquad (4)$$

Optical constants calculated from transmission spectra were used to calculate spectra simulated in D_2O for the same experimental conditions. These spectra are plotted as dotted lines in Figure 5. It is apparent that the relative intensities of the methyl and methylene stretching modes are different for the oriented and randomly organised molecules, which is a

qualitative indication that the tilt angle in the bilayer film is less than 55° (the "angle" corresponding to random orientation) from the surface normal.

Figure 7 shows the tilt angles of the symmetric and antisymmetric transition dipole moments as a function of applied electrode potential, along with the corresponding tilt angles of the hydrocarbon chains. The open shapes plot tilt angles for the Au|*h*-DMPE|*d*-DMPE film (tilt angles for the inner monolayer, adjacent to the Au surface) and the filled shapes plot tilt angles for the Au|*d*-DMPE|*h*-DMPE film (tilt angles for the outer monolayer, adjacent to the electrolyte). In the positive potential region, where the bilayer is expected to be directly adsorbed on the surface, the average tilt angle of the monolayer adjacent to Au is 15º and that of the monolayer adjacent to the electrolyte is 20º. At the negative potential limit, where the bilayer is likely to be separated from the surface by a layer of electrolyte,[7,9] the average tilt angles are closer: 14º and 16º for the Au|*h*-DMPE|*d*-DMPE film and Au|*d*-DMPE|*h*-DMPE film, respectively. These values are comparable with those obtained for DMPE films where both monolayers contain *h*-DMPE, ~17° from the surface normal.[14] Although the difference between the Au|*h*-DMPE|*d*-DMPE and Au|*d*-DMPE|*h*-DMPE films is small (compared with the estimated error of 3° arising from background subtraction), the tilt angle of the inner leaflet (adjacent to Au) is always smaller than that of the outer leaflet (adjacent to the electrolyte) in the potential region positive of the electrochemical phase transition. (The value of 17° obtained for Au|*h*-DMPE|*h*-DMPE films seems to be an average over the two layers.) The hydrocarbon chain tilt angle of DMPC bilayers was also higher for the electrolyte-facing leaflet.[12] This observation was attributed to modification of the inner leaflet structure by the gold surface because the tilt angle measured for the electrolyte-facing leaflet was consistent with that calculated from the molecular area at which the monolayer was transferred from the air|water interface.

If there is a water cushion between the DMPE layer and the surface at negative potentials, as observed for DMPC films,[9] the arguments made previously for the similarity in environment resulting in closer molecular orientation on each side of the bilayer (a difference of 5° compared with 10° at positive potentials)[12] could also apply to the case of DMPE, which also has similar tilt angles for the two monolayers at negative potentials. The closer to perpendicular orientation of DMPE hydrocarbon chains would also be consistent with the fact that the DMPE headgroup footprint occupies a comparable molecular area with the two chains. The fact that the electrolyte-facing monolayer has higher tilt angle than the gold-facing monolayer at positive potentials is more difficult to explain for DMPE because of its cylindrical shape. It is possible that there are differences in inter-headgroup interactions in each side of the bilayer. DMPE headgroups contain a hydrogen bond donor (the ammonium group) and a hydrogen bond acceptor (the phosphate group), as shown in Figure 1. The presence of both donor and acceptor enables the molecules to interact directly with one another via hydrogen bonding, as opposed to the water-mediated hydrogen bonding interactions between DMPC headgoups, which contain only hydrogen bond acceptors.[30] The tight hydrogen bonding network results in low mobility of the headgroups, observed previously for symmetric DMPE films, whose phosphate stretching absorptions were much narrower[14] than those of either DMPC[13] or DMPS. [15]. If the electrolyte disturbs this tight network, the headgroup orientation may differ between molecules directly adsorbed on Au and those in contact with electrolyte, in turn leading to a change in chain orientation. If this were the case, the electrolyte structure would have to alter at larger negative charge densities to account for the fact that the lower tilt angle (close to that of the Au-facing leaflet) is observed at negative charge densities. On the other hand, it is possible that the headgroups interact more strongly with the Au surface than with the electrolyte, as suggested for DMPC.[12] An alternative explanation could be that the deuterated chains of adsorbed

molecules have a slightly different tilt angle from hydrogenous chains or more fluidity and that the first, gold-facing layer influences the structure of the second, electrolyte-facing layer. Further studies to investigate this interpretation are in progress. The O-P-O (where O represents non-esterified oxygen atoms) symmetric stretching mode has slightly different orientation for hydrogenous and deuterated DMPE bilayers: *h*-DMPE spectra indicated higher tilt for this mode than *d*-DMPE spectra.[14] If the tilt angles of the symmetric and antisymmetric modes are similar for *h*-DMPE as they are for *d*-DMPE, the O-P-O plane lies flatter for *h*-DMPE than for *d*-DMPE, which is consistent with a smaller chain tilt angle for *h*-DMPE than *d*-DMPE. Alternatively, the differences may arise from variation in solvent content across the bilayer. The volume fraction of water in the electrolyte-facing monolayer has been shown to be greater in the positive potential range than that in the Au-facing monolayer for DMPE/DMPS (9:1 molar ratio) films formed from vesicles[20] so, although coverage of the surface by vesicles is not always as compact as from Langmuir transfer techniques, it is possible that the outer layer is more affected by solvent ingress than the inner.

There is a small variation in band intensity around the electrochemical phase transition, which was not apparent in the Au|*h*-DMPE|*h*-DMPE bilayers. The most likely explanation for this behaviour is that *d*-DMPE monolayers have more fluidity than *h*-DMPE monolayers. If the phase transition observed in the electrochemical measurements is indicative of water ingress, as for DMPC bilayers,[12] the ingress might be expected to lead to relative disorder in the layers, resulting in a slight increase in average tilt angle of the CH_2 groups (as some start to point in different directions if the chains twist). The disorder is slight in the hydrogenous leaflet as no trend is observed in IR band position. The isotherms in Figure 2 showed a greater fluidity of the deuterated molecules on a water subphase. Although the supported monolayers are notionally in the solid phase, there appears to be more flexibility within these

monolayers, which, in turn, translates to a slightly greater flexibility in the opposite monolayer. It is also possible that placing two layers of the same molecule leads to stronger inter-layer interactions than placing two layers of molecules with potentially different fluidty. These results show that the general, basic structure of the bilayers at equilibrium is generally unaffected but the dynamic behaviour of the bilayers is affected by deuteration. This observation could have implications for the use of deuterated analogues in determining separate signals for each monolayer in spectroscopy or for their use in neutron reflectivity measurements. The results do not suggest that data for hydrogenous and deuterated films are necessarily incomparable but rather that some care needs to be taken in their choice and comparison with homogeneously distributed bilayers would be prudent.

Conclusions

Selective isotopic substitution of hydrogen with deuterium has been used to study the two monolayers of Au-supported di-myristoyl phosphatidyl ethanolamine (DMPE) bilayers separately with in situ PM-IRRAS. The monolayers were found to have the same orientation at the most negative potentials and different orientation at potentials positive of the electrochemical phase transition. At these more positive potentials, the monolayer adjacent to Au was less tilted than the monolayer adjacent to the solution, as was observed previously for di-myristoyl phosphatidyl choline (DMPC) bilayers.[12] This result is attributed to a different interaction of headgroups with the Au surface or differences in orientation between deuterated DMPE and hydrogenous DMPE. A small variation in band intensity around the electrochemical phase transition was also observed for these asymmetric bilayers but was not observed previously for symmetric hydrogenous DMPE bilayers,[14] indicating that there may be slightly greater flexibility in the deuterated monolayer or a stronger interaction between two like monolayers. The results show that selective deuteration can have a small but

observable influence on dynamic behaviour of phospholipid films but the macroscopic barrier properties of the bilayers studied do not seem to be significantly altered.

Acknowledgements

EM is grateful to the School of Chemistry, University of Birmingham, for a studentship.

References

1. Pashley, R. M.; Karaman, M. E. *Applied Colloid Surface Chemistry*; Wiley: New York, 2004

2. Alberts, B.; Johnson, A.; Lewis, J.; Raff, M.; Roberts, K.; Walter, P. *Mol. Biol. Cell*, 4th ed.; Taylor and Francis: London, 2002, Chapter 10.

3. Sackmann, E. Supported membranes: Scientific and practical applications. *Science* **1996**, *271*, 43−48.

4. Guidelli, R.; Aloisi, G.; Becucci, L.; Dolfi, A.; Moncelli, M. R.; Buoninsegni, F. T. Bioelectrochemistry at metal | water interfaces. *J. Electroanal. Chem.* **2001**, *504*, 1−28.

5. Castellana, E. T.; Cremer, P. S. Solid-supported lipid bilayers: From biophysical studies to sensor design. *Surf. Sci. Rep.* **2006**, *61*, 429−444.

6. Andra, J.; Bohling, A.; Gronewold, T. M. A.; Schlecht, U.; Perpeet, M.; Gutsmann, T. Surface acoustic wave biosensor as a tool to study the interaction of antimicrobial peptides with phospholipid and lipopolysaccharide model membranes. *Langmuir* **2008**, *24*, 9148−9153.

7. Lipkowski, J. Building biomimetic membrane at a gold electrode surface. *Phys. Chem. Chem. Phys*. **2010**, *12*, 13874−13887.

8. Horswell, S. L.; Zamlynny, V.; Li, H.-Q.; Merrill, A. R.; Lipkowski, J. Electrochemical and PM-IRRAS studies of potential controlled transformations of phospholipid layers on Au(111) electrodes. *Faraday. Discuss*. **2002**, *121*, 405−422.

9. Burgess, I.; Li, M.; Horswell, S. L.; Szymanski, G.; Lipkowski, J.; Majewski, J.; Satija, S. Electric field-driven transformations of a supported model biological membrane: An electrochemical and neutron reflectivity study. *Biophys. J*. **2004**, *86*, 1763−1776.

10. Zawisza, I.; Lachenwitzer, A.; Zamlynny, V.; Horswell, S. L.; Goddard, J. D.; Lipkowski, J. Electrochemical and photon polarization modulation infrared reflection absorption spectroscopy study of the electric field driven transformations of a phospholipid bilayer supported at a gold electrode surface. *Biophys. J.* **2003**, *86*, 4055−4075.

11. Bin, X.; Zawisza, I.; Goddard, J. D.; Lipkowski, J. Electrochemical and PM-IRRAS studies of the effect of the static electric field on the structure of the DMPC bilayer supported at a Au(111) electrode surface. *Langmuir* **2005**, *21*, 330−347.

12. Garcia-Araez, N.; Brosseau, C. L.; Rodriguez, P.; Lipkowski, J. Layer-by-layer PMIRRAS characterization of DMPC bilayers deposited on a Au(111) electrode surface. *Langmuir* **2006**, *22*, 10365−10371.

13. Zawisza, I.; Bin, X.; Lipkowski, J. Potential-driven structural changes in Langmuir−Blodgett DMPC bilayers determined by in situ spectroelectrochemical PM IRRAS. *Langmuir* **2007**, *23*, 5180−5194.

14. Madrid, E.; Horswell, S.L. Effect of Headgroup on the Physicochemical Properties of Phospholipid Bilayers in Electric Fields: Size Matters. *Langmuir* **2013**, *29*, 1695−1708.

15. Madrid, E.; Horswell, S.L. Effect of Electric Field on Structure and Dynamics of Bilayers Formed From Anionic Phospholipids. *Electrochim. Acta* **2014**, in press.

16. Xu, S.; Szymanski, G.; Lipkowski, J. Self-assembly of phospholipid molecules at a Au(111) electrode surface. *J. Am. Chem. Soc*. **2004**, *126*, 12276−12277.

17. Sek, S.; Laredo, T.; Dutcher, J. R.; Lipkowski, J. Molecular resolution imaging of an antibiotic peptide in a lipid matrix. *J. Am. Chem. Soc*. **2009**, *131*, 6439−6444.

18. Li, M.; Chen, M.; Sheepwash, E.; Brosseau, C.L.; Li, H.Q.; Pettinger, B.; Gruler, H.; Lipkowski, J. AFM Studies of Solid-Supported Lipid Bilayers Formed at a Au(111) Electrode Surface Using Vesicle Fusion and a Combination of Langmuir-Blodgett and Langmuir-Schaefer Techniques. *Langmuir* **2008**, *24*, 10313−10323.

19. Chen, M.; Li, M.; Brosseau, C. L.; Lipkowski, J. AFM studies of the effect of temperature and electric field on the structure of a DMPC−cholesterol bilayer supported on an Au(111) electrode surface. *Langmuir* **2009**, *25*, 1028−1037.

20. Hillman, A. R.; Ryder, K. S.; Madrid, E.; Burley, A. W.; Wiltshire, R. J.; Merotra, J.; Grau, M.; Horswell, S. L.; Glidle, A.; Dalgliesh, R. M.; Hughes, A.; Cubitt, R.; Wildes, A. Structure and dynamics of phospholipid bilayer films under electrochemical control. *Faraday Discuss.* **2010**, *145*, 357−379.

21. Feng, Z. V.; Spurlin, T. A.; Gewirth, A. A. Direct visualization of asymmetric behavior in supported lipid bilayers at the gel-fluid phase transition. *Biophys. J.* **2005**, *88*, 2154−2164.

22. Xie, A. F.; Yamada, R.; Gewirth, A. A.; Granick, S. Materials science of the gel to fluid phase transition in a supported phospholipid bilayer. *Phys. Rev. Lett.* **2002**, *89*, 246103.

23. Leonenko, Z. V.; Carnini, A.; Cramb, D. T. Supported planar bilayer formation by vesicle fusion: the interaction of phospholipid vesicles with surfaces and the effect of gramicidin on bilayer properties using atomic force microscopy. *Biochim. Biophys. Acta* **2000**, *1509*, 131−147.

24. Dicko, A.; Bourque, H.; Pezolet, M. Study by infrared spectroscopy of the conformation of dipalmitoylphosphatidylglycerol monolayers at the air−water interface and transferred on solid substrates. *Chem. Phys. Lipids* **1998**, *96*, 125−139.

25. Tamm, L. K.; McConnell, H. M. Supported phospholipidbilayers. *Biophys. J.* **1985**, *47*, 105−113.

26. Crane, J. M.; Tamm, L. K. Role of cholesterol in the formation and nature of lipid rafts in planar and spherical model membranes. *Biophys. J.* **2004**, *86*, 2965−2979.

27. Hauser, H.; Pascher, I.; Pearson, R. H.; Sundell, S. Preferred conformation and molecular packing of phosphatidylethanolamine and phosphatidylcholine. *Biochim. Biophys. Acta* **1981**, *650*, 21−51.

28. Richer, J.; Lipkowski, J. Measurement of physical adsorption of neutral organic species at solid electrodes. *J. Electrochem. Soc.* **1986**, *133*, 121−128.

29. Lipka, G.; Chowdry, B. Z.; Sturtevant, J. M. A comparison of the phase transition properties of 1,2-diactylphosphatidylcholines and 1,2-diacylphosphatidylethanolamines in H_2O and D_2O. *J. Phys. Chem.* **1984**, *88(22)*, 5401-5406.

30. Casal, H.; Mantsch, H. H. Polymorphic phase behaviour of phospholipid membranes studied by infrared spectroscopy. *Biochim. Biophys. Acta* **1984**, *779*, 381−401.

31. Lewis, R. N. A. H.; McElhaney, R. N. Calorimetric and spectroscopic studies of the polymorphic phase behavior of a homologous series of n-saturated 1,2-diacyl phosphatidylethanolamines. *Biophys. J.* **1993**, *64*, 1081−1096.

32. Petersen, N. O.; Kroon, P. A.; Kainosho, M.; Chan, S. I. Thermal Phase Transition in Deuterated Lecithin Bilayers. *Chem. Phys. Lipids* **1975**, *14*, 343-349.

33. Barner, B. J.; Green, M. J.; Saez, E. I.; Corn, R. M. Polarization modulation Fourier-transform infrared reflectance measurements of thin-films and monolayers at metal-surfaces utilizing real-time sampling electronics. *Anal. Chem*. **1991**, *63*, 55−60.

34. Green, M. J.; Barner, B. J.; Corn, R.M. Real-time sampling electronics for double modulation experiments with Fourier-transform infrared spectrometers. *Rev. Sci. Instrum.* **1991**, *62*, 1426−1430.

35. Jackson, R.; Zamlynny, V. Optimization of electrochemical infrared reflection absorption spectroscopy using Fresnel equations. *Electrochim. Acta* **2008**, *53*, 6768−6777.

36. Zamlynny, V.; Lipkowski, J. In *Diffraction and Spectroscopic Methods in Electrochemistry*; Alkire, R. C., Kolb, D. M., Lipkowski, J., Ross, P. N., Eds.; Wiley-VCH: New York, 2006; Chapter 9.

37. Fresnel 1 software written by V. Zamlynny. E-mail: Vlad.Zamlynny@AcadiaU.ca.

38. Buffeteau, T.; Desbat, B.; Blaudez, D.; Turlet, J.M. Calibration procedure to derive IRRAS spectra from PM-IRRAS spectra. *Appl. Spectrosc.* **2000**, *54*, 1646-1650.

39. Zamlynny, V.; Zawisza, I.; Lipkowski, J. PM FTIRRAS studies of potential-controlled transformations of a monolayer and a bilayer of 4-pentadecylpyridine, a model surfactant, adsorbed on a Au(111) electrode surface. *Langmuir* **2003**, *19*, 132-145.

40. Helm, C. A.; Tippmann-Krayer, P.; Möhwald, H.; Als-Nielsen, J.; Kjaer, K. Phases of phosphatidyl ethanolamine monolayers studied by synchrotron X-ray-scattering. *Biophys. J.* **1991**, *60*, 1457−1476.

41.Ma, G; Allen, H.C. DPPC Langmuir monolayer at the air-water interface: probing the tail and head groups by vibrational Sum Frequency Generation Spectroscopy. *Langmuir* **2006**, *22*, 5341-5349.

42. Chung, J. B.; Hannemann, R.E.; Franses, E. I. Surface analysis of lipid layers at air/water interfaces. *Langmuir* **1990**, *6*, 1647-1655,

43. Liu, J; Conboy, J. C. 1,2-diacyl-phsophatidylcholine flip-flop measuredd directly by sum-frequency vibrational spectroscopy. *Biophys. J.* **2005**, *89*, 2522-2532.

44. Liu, J; Conboy, J.C. Direct measurement of the transbilayer movement of phospholipids by sum-frequency vibrational spectroscopy. *J. Am. Chem. Soc.* **2004**, *126*, 8376-8377.

45. Anglin, T. C.; Conboy, J. C. Kinetics and thermodynamics of flip-flop in binary phospholipid membranes measured by sum-frequency vibrational spectroscopy. *Biochemistry* **2009**, *48*, 10220-10234.

46. Brown, K. L.; Conboy, J. C. Lipid flip-flop in binary membranes composed of phosphatidylserine and phosphatidylcholine. *J. Phys. Chem. B* **2013**, *117*, 15041-15050.

47. Cameron, D. G.; Casal, H. L.; Mantsch, H. H. Characterization of the pretransition in 1,2-dipalmitoyl-sn-glycero-3-phosphocholine by Fourier transform infrared spectroscopy. *Biochemistry* **1980**, *19*, 3665−72.

48. Snyder, R. G.; Liang, G. L.; Strauss, H. L.; Mendelsohn, R. IR spectroscopic study of the structure and phase behavior of long-chain diacylphosphatidylcholines in the gel state. *Biophys. J.* **1996**, *71*, 3186−3198.

49. Snyder, R. G.; Hsu, S. L.; Krimm, S. Vibrational-spectra in C−H stretching region and structure of polymethylene chain. *Spectrochim. Acta A* **1978**, *34*, 395−406.

50. Umemura, J.; Cameron, D. G.; Mantsch, H. H. A Fourier transform infrared spectroscopic study of the molecular interaction of cholesterol with 1,2-dipalmitoyl-sn-glycero-3-phosphocholine. *Biochim. Biophys. Acta* **1980**, *602*, 32−44.

51. Mantsch, H. H.; Martin, A.; Cameron, D. G. Characterization by infrared spectroscopy of the bilayer to nonbilayer phase transition of phosphatidylethanolamines. *Biochemistry* **1981**, *20*, 3138−3145.

52. Casal, H. L.; Mantsch, H. H. The thermotropic phase behavior of N-methylated dipalmitoylphosphatidylethanolamines. *Biochim. Biophys. Acta* **1983**, *735*, 387−396.

53. Mantsch, H. H.; Hsi, S. C.; Butler, K. W.; Cameron, D. G. Studies on the thermotropic behavior of aqueous phosphatidylethanolamines. *Biochim. Biophys. Acta* **1983**, *728*, 325−330.

54. Okamura, E.; Umemura, J.; Takenaka, T. Fourier-transform infrared-attenuated total reflection spectra of dipalmitoylphosphatidylcholine monomolecular films. *Biochim. Biophys. Acta* **1985**, *812*, 139−146.

55. Mantsch, H. H.; McElhaney, R. M. Phospholipid phase transitions in model and biological membranes as studied by infrared spectroscopy. *Chem. Phys. Lipids* **1991**, *57*, 213−226.

56. Moskovits, M. Surface selection-rules. *J. Chem. Phys.* **1982**, *77*, 4408−4416.

57. Allara, D. L.; Swalen, J. D. An infrared reflection spectroscopy study of oriented cadmium arachidate monolayer films on evaporated silver. *J. Phys. Chem.* **1982**, *86*, 2700−2704.

58. Allara, D. L.; Nuzzo, R. G. Spontaneously organized molecular assemblies. 2. Quantitative infrared spectroscopic determination of equilibrium structures of solution-adsorbed n-alkanoic acids on an oxidized aluminium surface. *Langmuir* **1985**, *1*, 52−66.

59. Umemura, J.; Kamata, T.; Kawai, T.; Takenaka, T. Quantitative evaluation of molecular orientation in thin Langmuir−Blodgett films by FT-IR transmission and reflection−absorption spectroscopy. *J. Phys. Chem.* **1990**, *94*, 62−67.

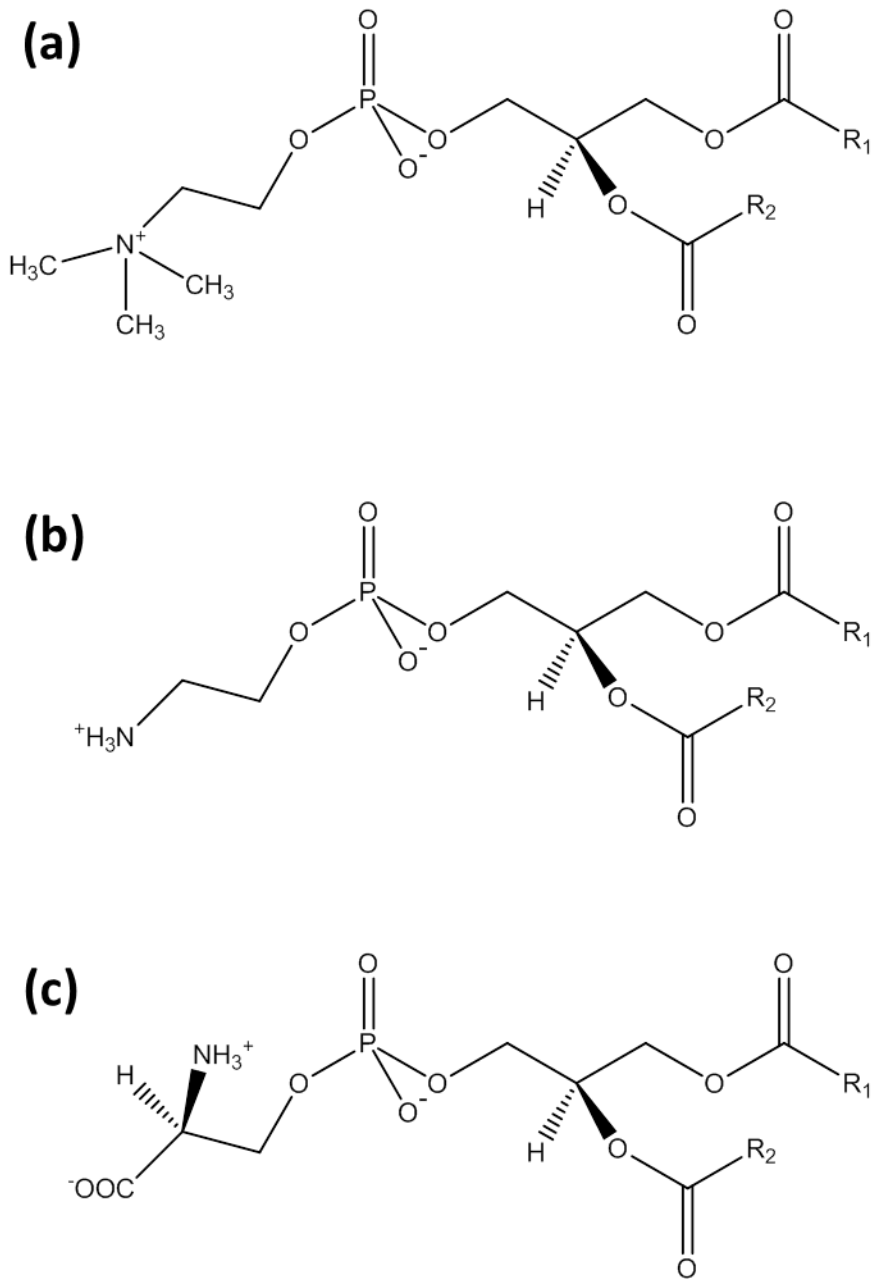

Figure 1 Chemical structures of the lipid types (a) phosphatidyl choline (PC), (b) phosphatidyl ethanolamine (PE) and (c) phosphatidyl serine (PS).

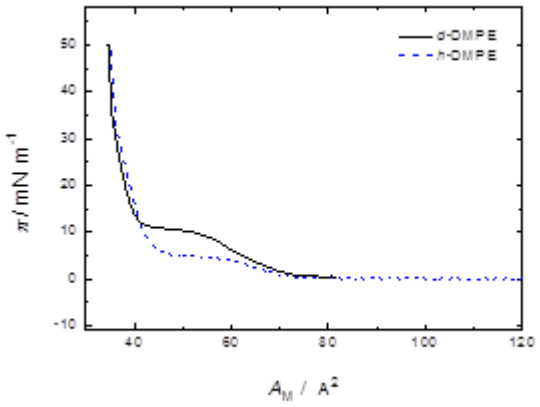

Figure 2 Pressure-area isotherms recorded for monolayers of *h*-DMPE (dotted line) and *d*-DMPE (solid line) on a water subphase at 19°C. The barrier speed was 25 cm^2 min^{-1}.

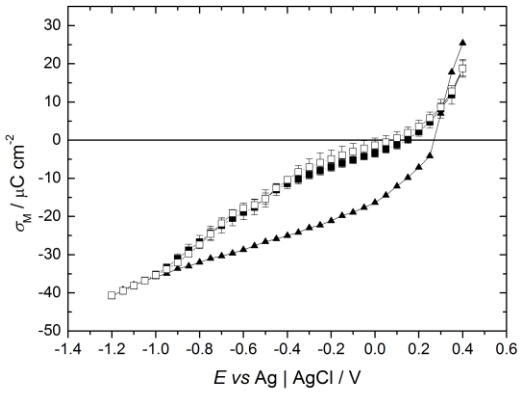

Figure 3 Charge density vs potential plots of Au in the absence of lipids (triangles), Au|h-DMPE,d-DMPE (open squares) and Au|d-DMPE|h-DMPE (filled squares).

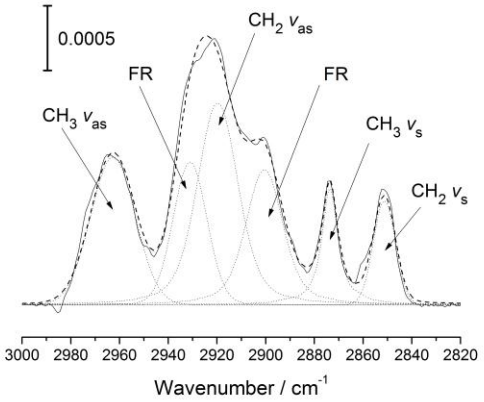

Figure 4 Example PM-IRRA spectrum of the C-H stretching region for a Au|*h*-DMPE|*d*-DMPE film, acquired at 0.0 V. Angle of incidence 51° and electrolyte (0.1 M NaF in D_2O) thickness 1.8 μm. The dotted lines show the fitted individual peaks and the dashed line shows the cumulative fit; the solid line represents the acquired data.

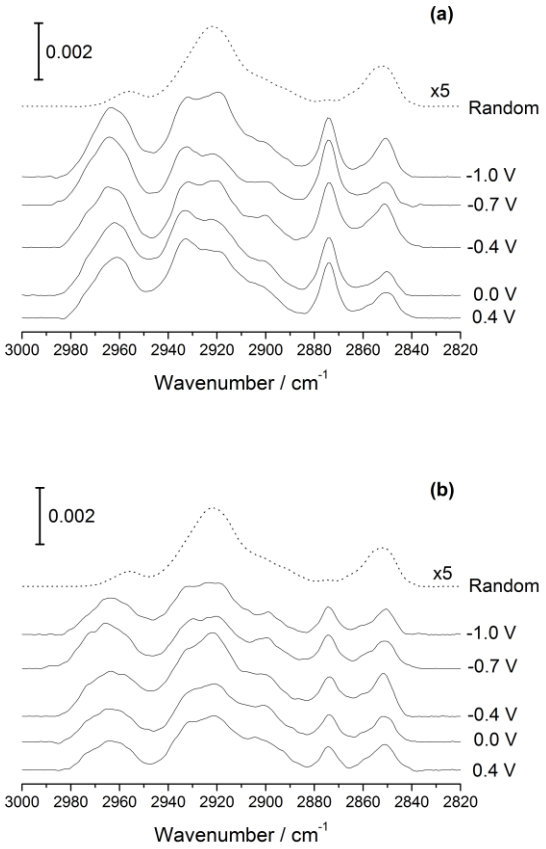

Figure 5 Selected PM-IRRA spectra acquired at various applied potentials of the C-H stretching region for (a) Au|d-DMPE|h-DMPE and (b) Au|h-DMPE|d-DMPE. Angle of incidence 51° and electrolyte (0.1 M NaF in D_2O) thickness 1.8 μm. The spectra are offset for clarity.

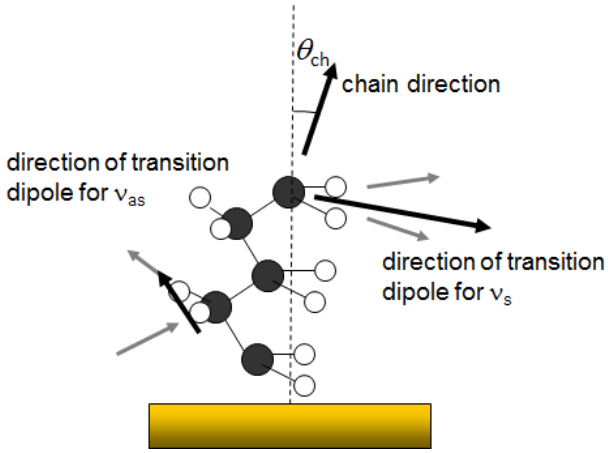

Figure 6 Schematic showing the directions of the transition dipoles corresponding to the symmetric and antisymmetric CH_2 stretching modes (black arrows) and their relationship with the chain tilt angle. The grey arrows show relative motions of the hydrogen atoms.

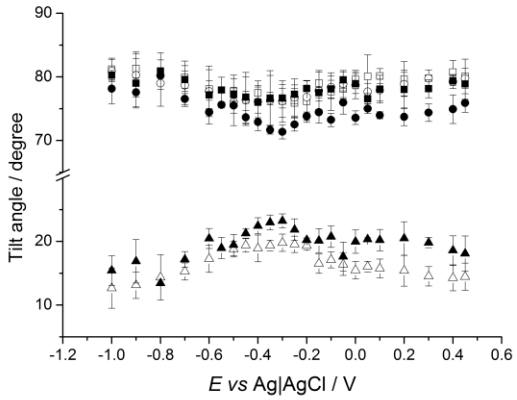

Figure 7 Squares: tilt angles of the transition dipoles corresponding to the symmetric CH_2 stretching modes: ■ Au|*d*-DMPE|*h*-DMPE, □ Au|*h*-DMPE|*d*-DMPE. Circles: tilt angles

of the transition dipoles corresponding to the antisymmetric CH_2 stretching modes. ● Au|*d*-DMPE|*h*-DMPE, ○ Au|*h*-DMPE|*d*-DMPE. Triangles: tilt angles of the hydrocarbon chains: ▲ Au|*d*-DMPE|*h*-DMPE, Δ Au|*h*-DMPE|*d*-DMPE. In each case, the error bars represent the standard deviations in tilt angles over three experiments.

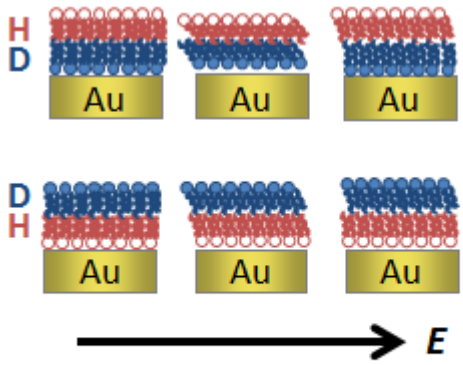

Table of Contents Graphic